General Disclaimer

One or more of the Following Statements may affect this Document

- This document has been reproduced from the best copy furnished by the organizational source. It is being released in the interest of making available as much information as possible.

- This document may contain data, which exceeds the sheet parameters. It was furnished in this condition by the organizational source and is the best copy available.

- This document may contain tone-on-tone or color graphs, charts and/or pictures, which have been reproduced in black and white.

- This document is paginated as submitted by the original source.

- Portions of this document are not fully legible due to the historical nature of some of the material. However, it is the best reproduction available from the original submission.

NASA CR-
150916

NAMRL-1228

NUCLEAR EMULSION MEASUREMENTS OF THE ASTRONAUTS' RADIATION EXPOSURE ON THE APOLLO-SOYUZ MISSION

Hermann J. Schaefer and Jeremiah J. Sullivan

NAVAL AEROSPACE MEDICAL RESEARCH LABORATORY

June 1976

Prepared for the
NATIONAL AERONAUTICS
AND
SPACE ADMINISTRATION

Approved for public release; distribution unlimited.

NUCLEAR EMULSION MEASUREMENTS OF THE ASTRONAUTS' RADIATION EXPOSURE ON THE APOLLO-SOYUZ MISSION

Hermann J. Schaefer and Jeremiah J. Sullivan

NASA Order No. T-81D

Approved by

Ashton Graybiel, M.D.
Assistant for Scientific Programs

Released by

Captain R.E. Mitchel, MC USN
Commanding Officer

23 June 1976

NAVAL AEROSPACE MEDICAL RESEARCH LABORATORY
PENSACOLA, FLORIDA 32508

SUMMARY PAGE

THE PROBLEM

On the Apollo-Soyuz mission each astronaut carried one passive dosimeter containing nuclear emulsions, plastic foils, TLD chips, and neutron-activation foils for recording radiation exposure. This report is limited to the presentation of data retrieved from nuclear emulsions.

FINDINGS

Protons, most of them trapped particles encountered in numerous passes through the South Atlantic Anomaly, contributed by far the largest share to the mission dose. Their LET spectrum was established from track and grain counts in G.5 emulsion for medium and high energies and from ender counts in K.2 emulsion for low energies. The total mission fluence of protons was found to be equivalent to a unidirectional beam of 448,500/cm^2. The broad spectrum was broken down into small LET intervals, which allowed application of constant mean LET and QF values for the computation of absorbed doses and dose equivalents. Their totals are 51 millirad and 74 millirem.

Counts of disintegration stars in K.2 emulsion are incomplete at report time. While a total of 467 stars has been identified, counting their prong numbers is still in progress. Applying the differential collision cross sections for the gelatin matrix and the silver bromide to the star count furnishes an estimated dose contribution from tissue stars and associated neutrons of 4.6 millirad and 38 millirem.

The population of HZE particles in one K.2 emulsion sheet was evaluated by estimating Z numbers and energies with the aid of reference tracks. Application of the QF/LET relationship of the International Commission on Radiological Protection and a constant QF of 20 beyond 1750 Mev/(g/cm^2T) furnished a HZE particle dose of 4.3 millirad and 61 millirem. Special events with extremely high LET values were recorded separately. Eight events of terminating particles with Z numbers of 10 and above and 15 through-shots of very heavy particles of high energies with Z numbers of 20 and above were found in an emulsion area of 1.5 square inch and 100 micron thickness.

ACKNOWLEDGMENT

The authors wish to acknowledge the expert technical assistance of Harold M. Arnold who operated the sectional microcamera and prepared the photomontages.

INTRODUCTION

The Apollo-Soyuz astronauts spent a total time of 216 hours in orbit from July 15 to July 24, 1975. While exposed to the space radiation environment, each crew member carried one passive dosimeter similar to the unit used on the Skylab missions. The dosimeter contained nuclear emulsions, plastic foils, thermoluminescent dosimeter chips, and neutron-activation foils. The following report is limited to the data retrieved from nuclear emulsions.

Although the radiation exposure on a 9-day near-Earth orbital mission was expected to be trivial, the results of the emulsion scans are of special interest because of the comparatively high orbital inclination of 52°, which distinguishes Apollo-Soyuz from all orbital missions of the Gemini and Apollo programs which had an orbital inclination of 30°. To be sure, the inclination of the Skylab orbit had also been 52°. However, the long duration of the Skylab missions had created problems in the evaluation of the emulsions because of track crowding and latent image fading. Quite differently, the comparatively short duration of the Apollo-Soyuz flight kept the background low, allowing retrieval of accurate quantitative data and a direct comparison to corresponding Gemini and Apollo missions.

The latter comparison is of special interest with regard to the galactic component of the radiation exposure. The lower geomagnetic cutoff at 52° as compared to 30° extends the spectrum accessible to the vehicle to lower energies, thereby substantially increasing total fluence. For the heavy component in particular the added low-energy section of the spectrum contains HZE particles which, by virtue of their low energies, reach the end of their ionization ranges within the vehicle. Such "enders" or near-enders constitute the specifically harmful type of event radiobiologically because of their very high LET values. Enders of HZE particles with Z numbers above about 10 have never been observed in the emulsions of the Gemini and orbital Apollo missions. Although still not so numerous as on lunar missions, they are a regular component of the track populations in the Apollo-Soyuz emulsions up to and including the $Z > 20$ class. This report presents micrographs of such enders as direct pictorial evidence for the basically different nature of the HZE particle exposure on a 52° as compared to a 30° orbit.

LET SPECTRUM, ABSORBED DOSE, AND DOSE EQUIVALENT OF PROTON EXPOSURE

The bulk of the proton fluence within the vehicle consists of trapped particles encountered in numerous passes of the South Atlantic Anomaly. Less frequent are protons originating as secondaries from nuclear collisions of high-energy primaries with the constituent nuclei of vehicle frame, equipment, and the body tissues themselves. As far as the astronaut's radiation exposure is concerned, a discrimination between the two types of protons is of no significance as long as the proton count correctly reflects the fluence entering the astronaut's body. The latter prerequisite is not fulfilled for secondary protons originating in nuclear disintegrations released in the heavy elements silver and bromine of the emulsion layer serving as sensor on the astronaut's body. It is fulfilled, though, for those secondaries from disintegration stars that are released in the constituent elements of the gelatin matrix of the emulsion since gelatin is a tissue-equivalent material. A distinction of the two types of protons originating in the emulsion can only be accomplished indirectly by applying the ratio of the interaction cross sections for gelatin and silver bromide to the total star count. It is therefore preferable to exclude all protons originating in stars within the emulsion from the evaluation of the proton dose and account for them later in the assessment of the tissue star dose in which also alpha particles and neutrons furnish substantial contributions.

Absorbed dose and dose equivalent of a proton exposure depend on the Linear Energy Transfer (LET) distribution of the particle fluence. LET is inversely related to energy. In emulsion the LET of a particle track is directly correlated to grain density. Therefore, determining the total number of proton tracks in an emulsion volume and grain-counting each track furnish complete information on the dose which the same track population would have produced in an equal volume of tissue as long as local attenuation processes in the emulsion do not significantly alter fluence and LET distribution. It is obvious that the latter proposition holds rigorously only for an infinitely thin emulsion layer. For a layer of finite thickness it would still hold for protons that lose only a negligible part of their total energy in the emulsion layer. However, as one proceeds to particles of lower energies, i.e., higher LET values, the fractional energy loss in emulsion can no longer be neglected. That means that the low-energy section of the spectrum as recorded in emulsion is no longer representative for the spectrum as it would prevail at the body surface without the emulsion layer covering it.

Because of the multidirectional incidence of radiation in space the critical energy below which (or LET above which) emulsion data do not correctly reflect the conditions in tissue cannot be defined rigorously since it strongly depends on the length of the trajectory in emulsion. This ambiguity can be avoided altogether by establishing the high-LET section of the distribution from the so-called ender count; i.e., from the frequency of protons ending within the emulsion layer. It is seen by inspection that this frequency, for equal volumes of emulsion and tissue, is directly proportional to the respective Stopping Powers of the two media independent of the angle of incidence. Correcting for the different media of sensor and target (emulsion and tissue) can be accomplished by a simple scaling factor. At the same time, the ender count bypasses the disadvantage of poor accuracy of the grain count for tracks of high LET resulting from the fact that the grains coalesce, in dense tracks, to blobs and long filaments. A further practical advantage is the more rapid accumulation of a statistically significant ender count because identifying enders requires much less scanning time than grain-counting the tracks.

The 50 micron G.5 emulsion 1B-2 was selected for establishing the LET distribution of the proton population from track and grain counts. The emulsion sheet had been developed in Amidol to a moderate level. For establishing the calibration curve relating grain density to LET for this particular emulsion layer, three long proton enders were grain-counted and the dependence of grain density on residual range in emulsion determined. The mean values of the uncorrected raw scores for the three enders are shown in Figure 1* as circled dots. The smooth curve of best fit in the same figure was used for converting grain density to LET. The range/LET and range/E functions for protons in G.5 emulsion as tabulated by Barkas (1) were used. Figure 2 shows the LET/grain density curve as it follows from the indicated procedure. Of crucial importance is the minimum grain density g_o = 19 grains/100μ Em since it determines the slope of the initial recti-linear section of the calibration curve. This anchor point was determined from tracks of minimum grain density in a control emulsion processed together with the flown emulsion. Because of the very low background, tracks of minimum density could be easily identified in this emulsion.

For the track and grain count analysis of the flown emulsion an area in the central region of the emulsion sheet was selected and pre-examined beforehand at low power to ensure that no disintegration stars were in proximity that could feed spurious star prong protons into the counted volume. A total of 893 track segments were grain-counted and their three-dimensional lengths

---

* In order not to break the continuity of the text, all tables and illustrations appear at the end.

measured and corrected for unprocessed emulsion. Scanning was conducted with a 90x objective and 10x eye pieces. Grain density was resolved up to about 200 gr/100μEm. Tracks with still higher counts were classified as black tracks and analyzed merely with regard to their length in order to establish the grand total fluence. The exact configuration of the LET distribution was determined only up to 140 gr/100μEm, corresponding to an energy of 15 Mev and an LET of 33.1 Mev/(g/cm^{2}T). This limitation was imposed in order to avoid the rather large error incurred in grain counts in the region of beginning saturation. However, the cut-off was of no consequence for the determination of the total dose because as mentioned before, the dose contribution from the high-LET section was established from the ender count.

Table I presents the results of the track and grain count analysis. Column 1 shows grain density classes, Column 2 the corresponding classes of LET in tissue. Grain densities have been converted to LET in emulsion according to the curve in Figure 2. LET has been converted from emulsion to tissue according to the tables published by Janni (2). Differential fluences shown in Column 3 reflect directly the raw scores of segment length totals in the respective classes. The totals are expressed in terms of the equivalent unidirectional fluence which would produce, in the scanned emulsion volume, the same total track length as actually observed. Column 4 shows the cumulative sums of the differential fluences in Column 3; in other words, it defines the integral LET spectrum. Figure 3 shows the spectrum as a semilog plot; as mentioned before, the spectrum has been defined from the track and grain count scores only up to the LET of 33.1 Mev/(g/cm^{2}T) as indicated by the uppermost point in the graph. For the evaluation of dose the LET spectrum has been used up to the LET of 46 Mev/(g/cm^{2}T), indicated in Figure 3 by an arrow. The dose was computed by breaking down the interval into 56 sections, and establishing differential fluence and mean LET for each section from the smooth curve in Figure 3. Applying the relationship: 1 Mev per gram tissue = 0.016 microrad to the 56 fractions leads to a total dose of 38.8 millirad.

As mentioned before, the balance of the toral proton dose contributed by the high-LET section of the spectrum was established from the ender count in emulsion corrected for the different Stopping Powers of the two media. Counts of proton tracks entering the emulsion layer from the outside yet ending within were conducted in K.2 emulsions of the three packs. Scanning for enders was conducted with a 53x objective and 10x eye pieces. All enders were traced back to their origin and rejected when they were identified as star prongs or so-called suspended tracks (one-prong "stars" or neutron recoils).

The results of the ender counts are presented in Table II. Rounding the count for Pack 1B off to 28/mm^2 for a 200 micron emulsion layer, we arrive at the corresponding tissue dose in the following way: Since the dose from minimum LET to 46 Mev/(g/cm^{2}T) is determined from the track and grain count analysis in the G.5 emulsion, the dose contribution from the enders has to be evaluated for the interval from 46 to 890 Mev/(g/cm^{2}T). 46 Mev/(g/cm^{2}T) corresponds to an energy of 10 Mev and residual ranges of 562 micron in emulsion or 1370 micron in tissue. In the energy interval from zero to 10 Mev, the Stopping Power ratio of emulsion to tissue varies from 1.7 to 2.2. If we assume a mean ratio of 2.0, the quoted count in emulsion corresponds to 14/mm^2 for a 200 micron layer of tissue or 70,000/cm^3 tissue. Each ender contributes an absorbed energy of 10 Mev to the dose, and the contribution has to be analyzed with regard to its LET distribution in order to establish the corresponding QF distribution for evaluation of the dose equivalent. For this purpose the interval was broken down into 26 sections. Constant mean LET and QF values were applied to each section. The totals of the 26 contributions were found to be 12.1 millirad and 35.6 millirem. Adding the contribution from the LET spectrum below 46 Mev/(g/cm^{2}T) for which QF can be set equal to 1.0, we obtain a grand total proton dose of 50.9 millirad or 74.4 millirem for the Apollo-Soyuz mission. The values define a mean QF of 1.46.

Figure 4 attempts to demonstrate pictorially the track and grain count and the ender count methods. The upper six micrographs show fields randomly selected from the general area of the G.5 emulsion where track and grain counts have been conducted. It should be pointed out though that the micrographs have been taken with a 53x objective whereas in actual counting a 90x objective has been used. However, the depth of sharp focus of a 90x objective is so small that a still picture with constant depth of focus reveals only very few details.

The long field at the bottom of Figure 4 shows two proton enders in K.2 emulsion. Because of its low sensitivity, the K.2 emulsion suppresses the general background as well as proton tracks of medium and high energies so much that proton enders with their characteristic waviness due to small-angle nuclear scattering stand out conspicuously, and scanning can be conducted rapidly with a 53x objective. It should be mentioned that the proximity of the two enders in Figure 4 is a rare coincidence for the small fluence of enders on Apollo-Soyuz, which corresponds to a mean frequency of slightly less than one per two visual fields.

DOSE CONTRIBUTION FROM TISSUE DISINTEGRATION STARS

A sizeable fraction of the total mission dose is produced by secondaries released in nuclear interactions which appear as stars in nuclear emulsion. Evaporation stars constitute by far the most common type of interaction event. Their secondaries, mostly protons, neutrons, and alpha particles, center heavily on the energy interval from a few to about 50 Mev. That means that they deposit their total energy locally. As mentioned earlier, nuclear emulsion is not a tissue-equivalent material; therefore, the star population is not directly representative of the tissue dose. Merely those stars which originate in the gelatin matrix of the emulsion reflect the tissue dose. Two indirect methods exist for determining the fraction of the total star population produced in the gelatin. The first method divides the total star frequency into the fractions originating in silver bromide and gelatin by applying the respective cross sections for nuclear interaction. The second method does essentially the same graphically by evaluating the change of slope of the integral prong-number spectrum of the total star population. Both methods have been proposed by Birnbaum and co-workers (3). Davison (4) has studied the prong-number spectrum of stars in emulsion exposed to galactic radiation. He proposes a representative mean gelatin star that has 3.7 prongs, a mean energy of 14 Mev per prong, and a mean QF of 6.5. Inasmuch as Davison has conducted his analysis specifically for assessing personnel exposure, his model appears a very appropriate choice in the present context.

At the time this report is being written, data on the star population are still incomplete. While a total of 467 stars have been located, prong number counts are still in progress. This deprives us of the possibility of verifying the results of the cross section method with the change-of-slope test. We nevertheless proceed with the first-mentioned method in order to establish a preliminary result, which we hope to put on a firmer basis by the time the complete prong spectrum becomes available.

Division of the total number of 467 stars by the scanned emulsion volume furnishes a star frequency of 6500 stars/ccE . The relative interaction cross sections for total emulsion, silver bromide, and gelatin are 1.36, 1.00, and 0.36, respectively. Applying the ratio of 0.36/1.36 to 6500 stars furnishes 1720 stars originating within the gelatin matrix. Since the matrix occupies about one half of the total volume of unprocessed emulsion, we arrive at a frequency of 3442 stars/cc gelatin. Evaluating these stars in terms of the standard model proposed by Davison, we obtain doses of 2.58 millirad and 18.1 millirem as the contribution of tissue disintegration stars to the mission dose.

The frontispiece facing the title page of this report shows a typical disintegration star with 23 prongs. The large prong number identifies the star as a silver or bromine disintegration. That means it represents an event that could not be released in tissue. However, the star illustrates well the multiple production of secondaries in nuclear interactions of high-energy primaries with nuclei of local material.

Davison's model of a standard emulsion star considers only visible prongs; i.e., more specifically, protons and alpha particles. However, disintegration stars also constitute a prolific source of neutrons. Powell, Fowler, and Perkins, in their classical study on the nuclear emulsion method (5), present prong-generation spectra for the neutrons, protons, and alpha particles of cosmic-ray induced evaporation stars, suggesting a neutron to proton-plus-alpha ratio of 4.1 to 5.9. Applying this ratio to the mean prong number of 3.7 per star for Davison's model, we obtain a mean number of 2.57 neutrons per star. Assuming again a mean energy of 14 Mev per particle, we arrive at a neutron dose of 1.98 millirad or 19.8 millirem. Adding to it the contributions from protons and alpha particles, we obtain a total tissue star dose of 4.56 millirad or 37.9 millirem. Finally, going back to the preceding section where a total proton dose of 50.9 millirad or 74.4 millirem has been derived, we find a total mission dose of 56 millirad or 112 millirem, corresponding to a mean QF of 2.0. These values still do not present the grand-total mission dose because they do not contain the contribution from HZE particles. However, since a certain fraction of the latter contribution cannot adequately be measured in units of millirad or millirem, we treat the emulsion data on the heavy component as a completely separate entry in the account of the astronauts' radiation exposure.

HZE PARTICLE EXPOSURE

As mentioned already in the Introduction, the HZE particle exposure on Apollo-Soyuz was basically different from those on earlier Gemini and orbital Apollo missions because of the higher orbital inclination of 52° as compared to 30°. Due to the higher inclination the cut-off of the spectrum was extended downward so much that low-energy particles were admitted that were able to reach the end of their ionization ranges before being fragmented in nuclear collisions. Such enders or thindowns, as they are sometimes called because of their characteristic dagger-like appearance in emulsion, are of special radiobiological significance because they presumably produce, due to their extremely high LET, in the microstructure of tissue a special type of lesion for which no counterpart exists in conventional nuclear radiations.

Because of their just-described unique optical appearance, enders stand out conspicuously and can easily be distinguished. Figure 5 demonstrates the typical features. It shows selected segments of a track produced by a particle of estimated Z = 8-10 that traversed four emulsion sheets of the stack in Pack 2B. The micrograph at the far right shows the track in the 100 micron K.2 emulsion #3. It travelled from there through the 25 micron G.5 emulsion #4 (not shown), then through the 50 micron G.5 #5 (second from right), and finally entered the 100 micron K.2 #6 where it came to rest. The three micrographs to the left show the coherent terminal segment of the track broken into three parts for easier presentation. Examining the terminal segment at the far left, we see that, in the upper part, delta rays of short range still branch out from the solid core, becoming even shorter as the particle slows down further and finally disappearing completely so that the tail end assumes sharp contours. Quite differently, the four other segments in Figure 5 show little if any structural change along their respective lengths.

The uniquely different appearance of the terminal section at the far left in Figure 5 is the essential clue for identification of enders or thindowns in the scanning process. It should be

mentioned in this connection that the core diameter of a track does not directly indicate LET because it depends upon the speed of the particle and not upon its LET. Peak LET of the particle in Figure 5 acutally occurs only some 20 micron upbeam from the very end of the track. It is seen then that the specifically harmful section of a track where LET passes through a maximum can be identified unambiguously by its sharp convergent contours. Such identification poses no problems even if the terminal section of a track is not completely contained within the emulsion layer. Two examples of such near-enders are shown in Figure 6. To the left we see a track of an estimated Z = 8-10 and to the right one of an estimated Z = 12-14. Although the very tips of the tails are missing in both segments, it is clearly seen that the particles must have come to rest a few micron farther downbeam. The track in the center of Figure 6 is added for the purpose of comparison; it represents a track of high energy and an estimated Z = 14-16. The three track segments in Figure 6 were taken from 100 micron K.2 emulsions. Because of its lower sensitivity the K.2 emulsion suppresses somewhat the delta ray auras of tracks of high energy. However, as Figure 6 demonstrates, the distinction of enders and near-enders from high-energy tracks is not impaired.

G.5 emulsion with its higher sensitivity and its larger grain size allows a better differentiation of the delta ray auras of medium and high-energy tracks. Figure 7 shows examples of tracks of very high energies in G.5 emulsion. All three are taken from the 50 micron G.5 #1 in Pack 2B. From left to right estimated Z numbers are 18-20, 16-18, and 12-14. At the same time the micrographs show the heavier background resulting from the higher sensitivity of the G.5. Figure 8 shows three heavy tracks of high-energy particles in 100 micron K.2 emulsions. Estimated Z numbers from left to right are > 20, 14-16, and 12-14.

Determination of precise Z numbers and LET values of HZE particle tracks requires long segments and the tracing of individual particles through several emulsion layers for establishing a statistically significant delta ray count and its gradual change with residual range. Since particles of Z numbers above about 8 or 10 are comparatively infrequent as such, throughshots of the indicated kind are very rare events in the few emulsion sheets of small size in a personnel dosimeter pack. However, semi-quantitative estimates can be made by grading short track segments with the aid of reference standards whose Z numbers and LET values or energies are accurately known. The Z estimates shown in the illustrations were made by using standard tracks from the monograph of Powell, Fowler, and Perkins (5) already referred to in a different context above.

We have conducted such Z and E estimates for the total population of heavy tracks in one complete emulsion sheet. The 100 micron K.2 emulsion 3B-3 of 1x1½ inch size was selected for this purpose. In a preliminary run with a 10x objective all tracks to be graded were located with their x and y coordinates. In two final runs with 25x and 53x objectives track appearance was compared for assessment of Z and E values. Energy was estimated according to the appearance of the delta ray aura. A vestigial aura was rated "Low", a normally developed, "Medium", and a strongly developed, "High". Z numbers were estimated by the reference standards mentioned above (5), and by attempting a balanced compromise between core thickness and delta ray aura. For the determination of LET the energy ratings L, M, and H were considered as reflecting particle energies corresponding to 6x, 4x, and 2x minimal LET. The values themselves were obtained by multiplying the LET of protons by Z^2.

Table III presents the results of the scan and the indicated conversion. The dose contributions from the three E categories have been consolidated in the table into one value for each Z class. Absorbed doses have been converted to dose equivalents, using the QF/LET relationship recommended by the International Commission on Radiological Protection (ICRP).

The recommendations define a QF of 20 for 1750 Mev/(g/cm^{2}T) and do not contain specifications for still higher LET values. We have applied, in computing the doses in Table III, to all LET values above 1750 Mev/(g/cm^{2}T) a constant QF of 20. We are entirely aware that this is not a radiobiologically meaningful approach since it is generally agreed that somewhere above (or possibly even slightly below) the just-quoted LET, a limit is reached beyond which conventional dosimetric concepts and units cease to be valid. We expressly present the data in Table III for the purpose of demonstrating that on an Apollo-Soyuz type mission, HZE particle exposure, even if evaluated in conventional terms, represents a sizeable contribution. The prospect that a certain fraction of it might possess a unique effectiveness of a yet unexplored nature would seem to call all the more for careful record keeping. With this situation in mind, we have set aside, in conducting the scan for HZE particles, all track segments with extremely high-LET values and have classified them as "Special Events". Two types of events were distinguished: heavy tracks with convergent contours void of delta rays, indicating enders and near-enders with estimated Z numbers of 10 and higher; tracks with very heavy cores and well-developed delta ray auras, indicating Z numbers of 20 and higher. In the scanned emulsion sheet of 1.5 square inch area and 100 micron thickness, 8 events of the first type and 15 of the second type were identified. The near-enders in Figure 6 illustrate the first kind; the left and center track in Figure 8 the second. While the Z estimates carry a certain margin of error, the indicated frequencies should establish at least a lower limit for the frequency of events with exceptionally high local energy densities.

CONCLUSION

The reported findings concerning the Apollo-Soyuz astronauts' radiation exposure as such do not contain anything out of the ordinary that would seem to require special attention. However, in regard to the suitability of nuclear emulsion as a recording medium in operational space radiation dosimetry, a comparison of the results with those for the Skylab missions reported earlier (6) appears of interest. Essentially identical personnel dosimeters have been flown on both kinds of missions. Comparing the data for the long-duration Skylab flights with those for the 9-day Apollo-Soyuz flight, we become aware of the fact that track crowding and latent image fading imposed severe limitations to the retrieval of accurate quantitative information from the Skylab emulsions, whereas both problems were not encountered at all on Apollo-Soyuz. These findings once more confirm the conclusion already drawn in the Skylab report (6) that nuclear emulsion is a very adequate sensor for missions of 1-to-2 week duration. In fact, it appears to be the ideal recording medium since it is commercially available in a variety of sensitivities with a uniformity in quality that can be achieved only in large-scale industrial production. Nuclear emulsion has been used extensively by cosmic ray physicists for more than 25 years and for more than 20 years in industrial neutron radiation safety monitoring. It seems a logical step to combine the large experience in both areas and to utilize it for developing a dosimetric system for the Space Shuttle. From the standpoint of legal requirements for ensuring radiation safety for Shuttle crews and passengers, nuclear emulsion has the distinct advantage of providing permanent documentation of radiation exposure in space. While immediately after completion of a mission a brief spot-check often suffices for compliance with regulations, a thorough re-examination and detailed track counts can be conducted at any later time in order to refute unfounded claims of radiation damage.

REFERENCES

1. Barkas, W.H., Nuclear Research Emulsions. I. Techniques and Theory. New York: Academic Press, 1963.

2. Janni, J.F., Calculations of energy loss, range, pathlength, straggling, multiple scattering and the probability of inelastic nuclear collisions for 0.1-1000 Mev protons. AFWL-TR-65-150. Kirtland Air Force Base, New Mexico: Air Force Weapons Laboratory, 1966.

3. Birnbaum, M., Shapiro, M.M., Stiller, B., and O'Dell, F.W., Shape of cosmic-ray star-size distributions in nuclear emulsions. Phys. Rev., 86: 86-89, 1952.

4. Davison, P.J.N., Radiation dose rates at supersonic transport altitudes. M.O.A. Grant PD/34/017. Farnborough, Hampshire, England: Royal Aircraft Establishment, 1967.

5. Powell, C.F., Fowler, P.H., and Perkins, D.H., The Study of Elementary Particles by the Photographic Method. New York: Pergamon Press, 1959.

6. Schaefer, H.J., and Sullivan, J.J., Nuclear emulsion measurements of the astronauts' radiation exposures on Skylab Missions 2, 3, and 4. NAMRL-1220. Pensacola, Fla: Naval Aerospace Medical Research Laboratory, 1975.

Table I

Results of Track and Grain Count Analysis of Proton Track Population in G.5 Emulsion 1B-2 on Apollo-Soyuz

Grain Density, gr/100 micron Em	LET, Mev/(g/cm^{2}T)	Equiv. Unidirect. Fluence, Protons/cm^2	Pr/cm^2 ≤ LET	log LET, Upper Lmt.
< 20	< 2.21	52,910	52,910	0.344
20-29	2.21-3.33	118,080	170,990	0.522
30-39	3.33-4.32	79,130	250,120	0.636
40-49	4.32-5.60	47,240	297,360	0.748
50-69	5.60-8.35	68,950	366,610	0.922
70-89	8.35-11.65	40,660	406,970	1.066
90-119	11.65-20.9	25,050	432,020	1.320
120-140	20.9-33.1	6,890	438,910	1.520
> 140	33.1-890	9,610	448,520	2.950

Table II

Results of Proton Ender Counts in K.2 Emulsions on Apollo-Soyuz

Pack No.	Crew Member	Total N counted	N/mm^2 in 200 micron K.2
1B	CMDR	101	27.9
2B	C PILOT	101	25.7
3B	D PILOT	105	25.0

Table III

Results of HZE Particle Scan in K.2 Emulsion
3B-3 on Apollo-Soyuz

Estimated Z Number	Identified Segments, N	Total L, cm/cm² T	Dose	
			millirad	millirem
2-4	1390	386.90	0.776	2.514
4-6	296	85.64	0.495	3.824
6-8	136	37.95	0.399	4.731
8-10	96	27.31	0.431	6.627
10-12	111	26.11	0.582	10.781
12-14	72	19.69	0.677	13.432
14-16	35	11.53	0.534	10.682
16-18	8	2.70	0.154	3.057
18-20	10	3.84	0.273	5.464
		Total:	4.321	61.112

23 track segments with very high LET values, 8 of them heavy enders or near-enders, are not included in this table.

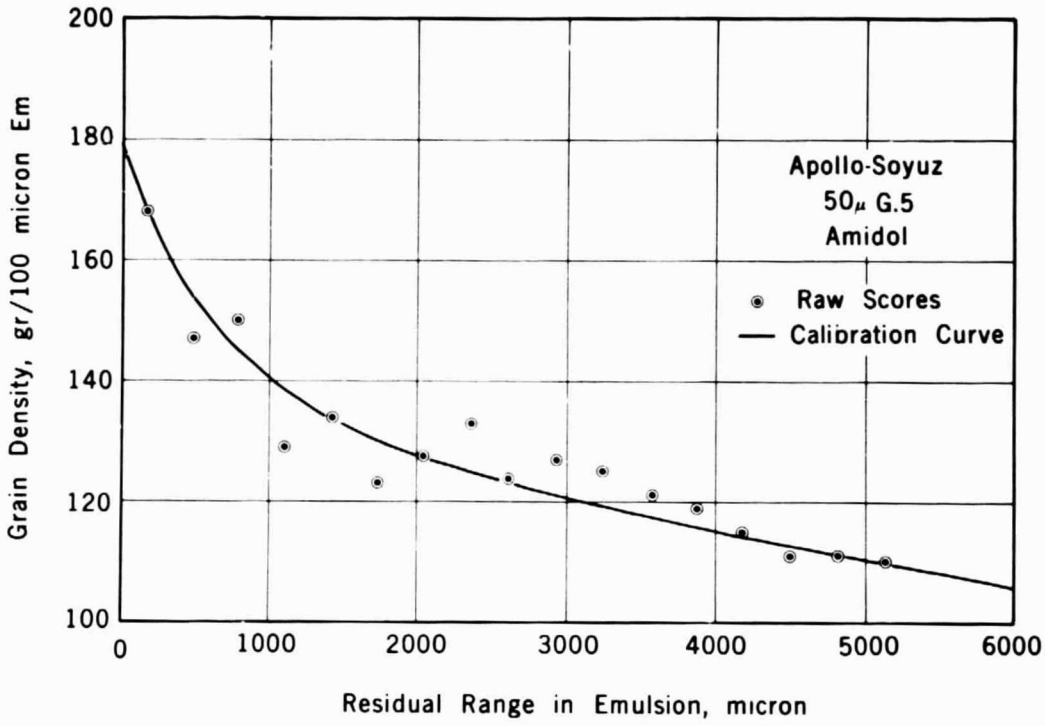

Grain Density/Range Function for Proton Enders
in G.5 Emulsion 1B-2 Flown on Apollo-Soyuz

Figure 1

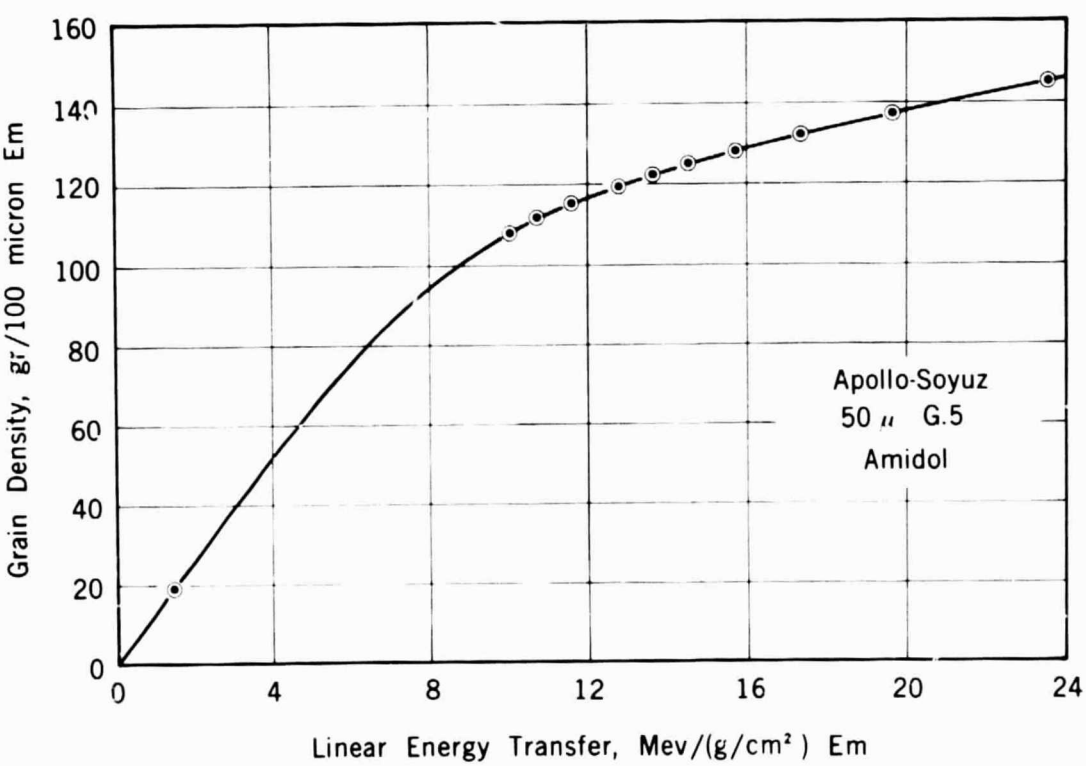

Grain Density/LET Calibration for Emulsion 1B-2 Flown on Apollo-Soyuz

Figure 2

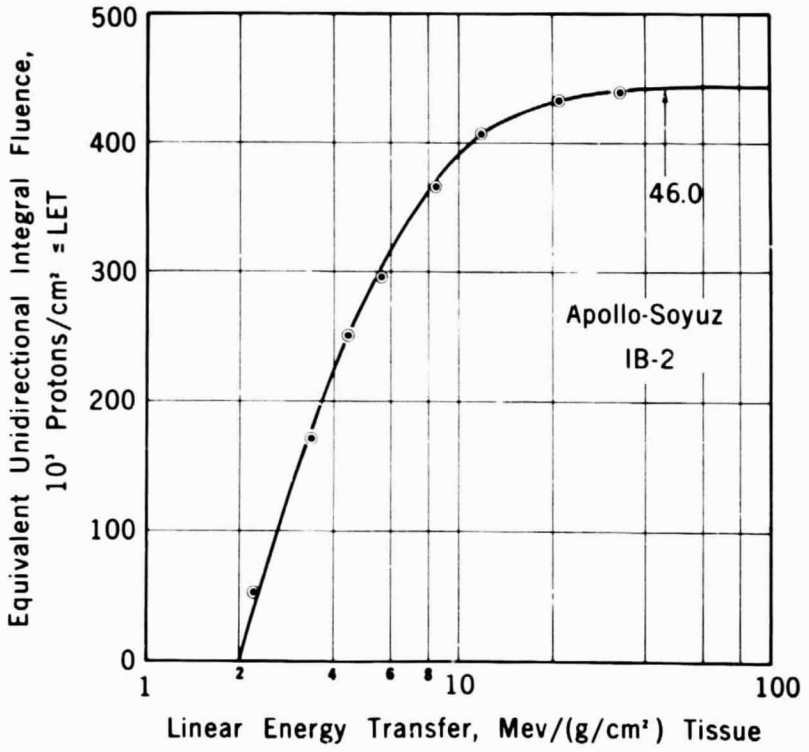

Integral LET Spectrum of Proton
Exposure on Apollo-Soyuz

Figure 3

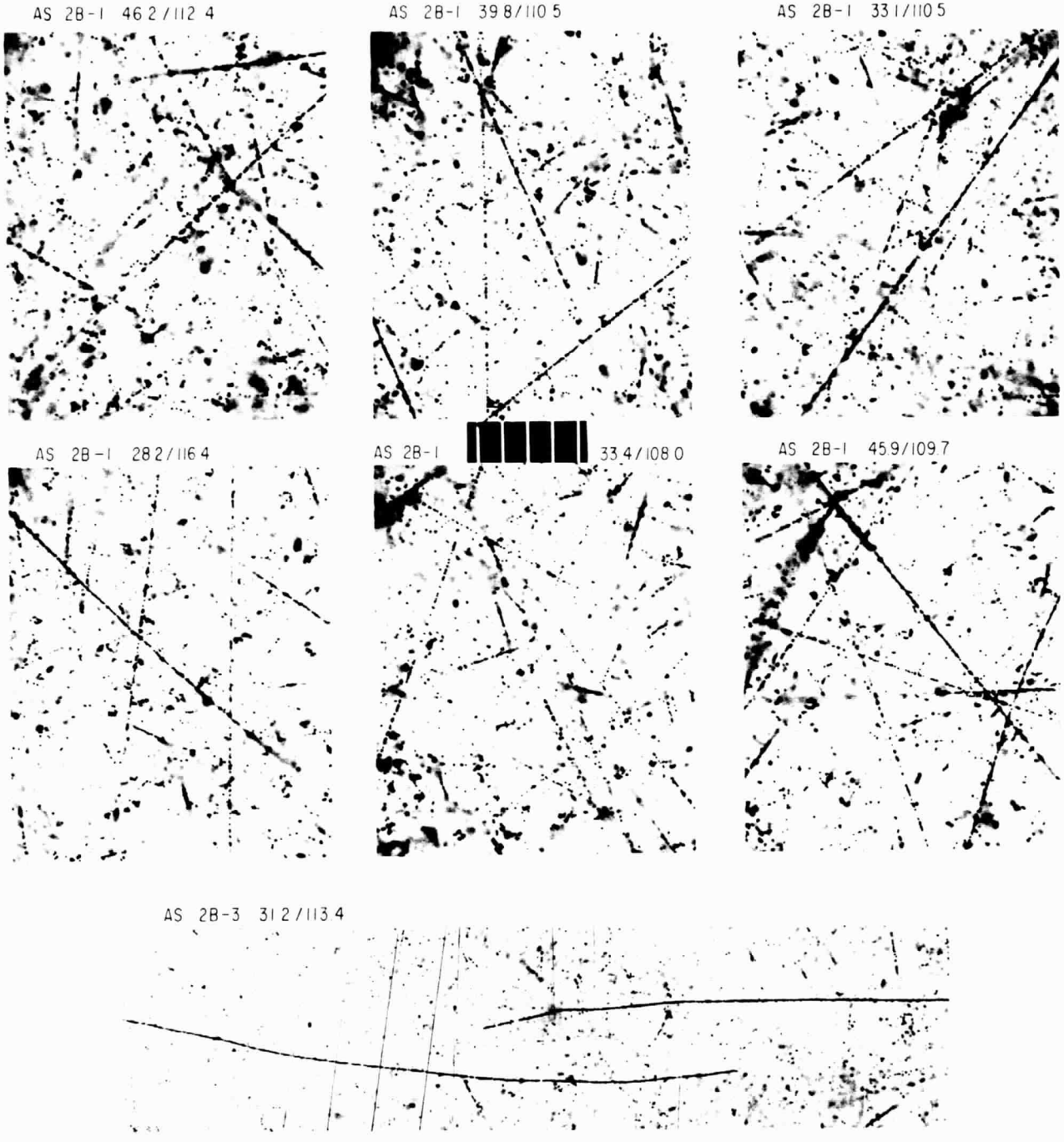

1 Div = 10μ

Proton Tracks in Apollo-Soyuz Emulsions

Square Fields: Tracks of Medium and High Energies in G.5 Emulsion

Long Field: Two Proton Enders in K 2 Emulsion

Figure 4

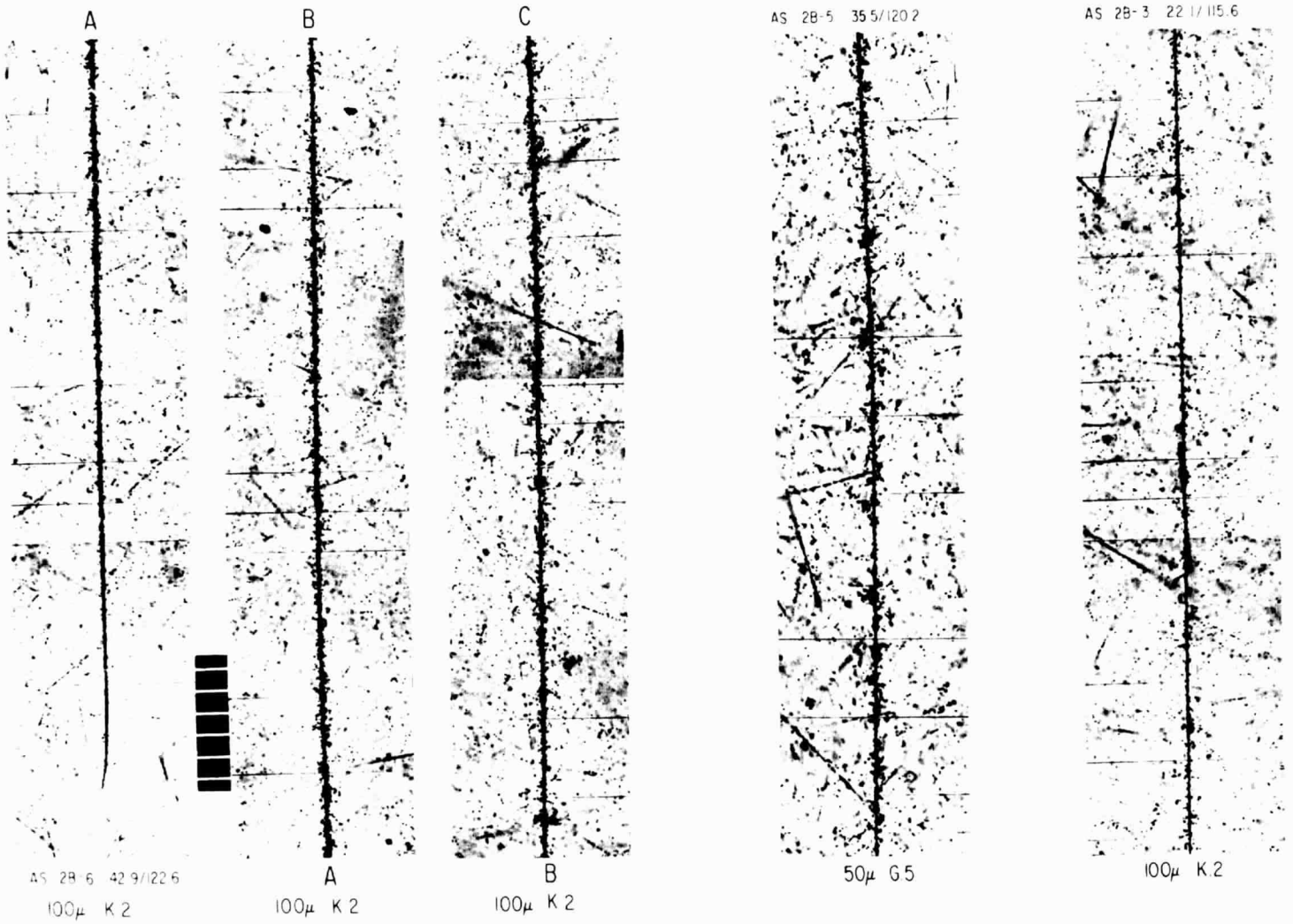

Selected Track Segments of HZE Particle of Z = 8 Traversing Four Emulsions in Pack 2B (CM Pilot) on Apollo - Soyuz

Figure 5

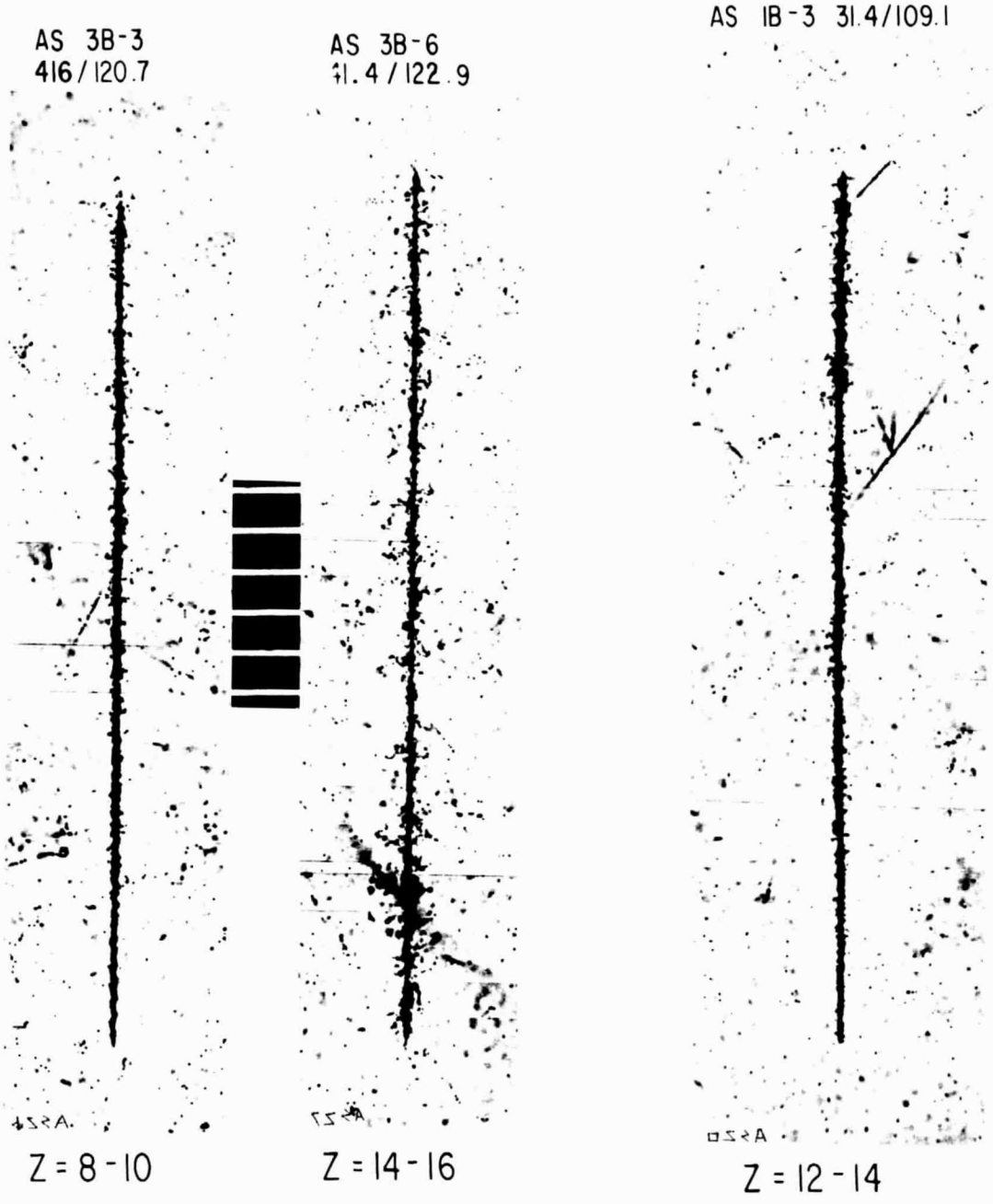

Near-Enders (left & right) and High-Energy Track in 100μ K.2 Emulsions Flown on Apollo-Soyuz.
(left & center: D Pilot; right: Cmdr.)

Figure 6

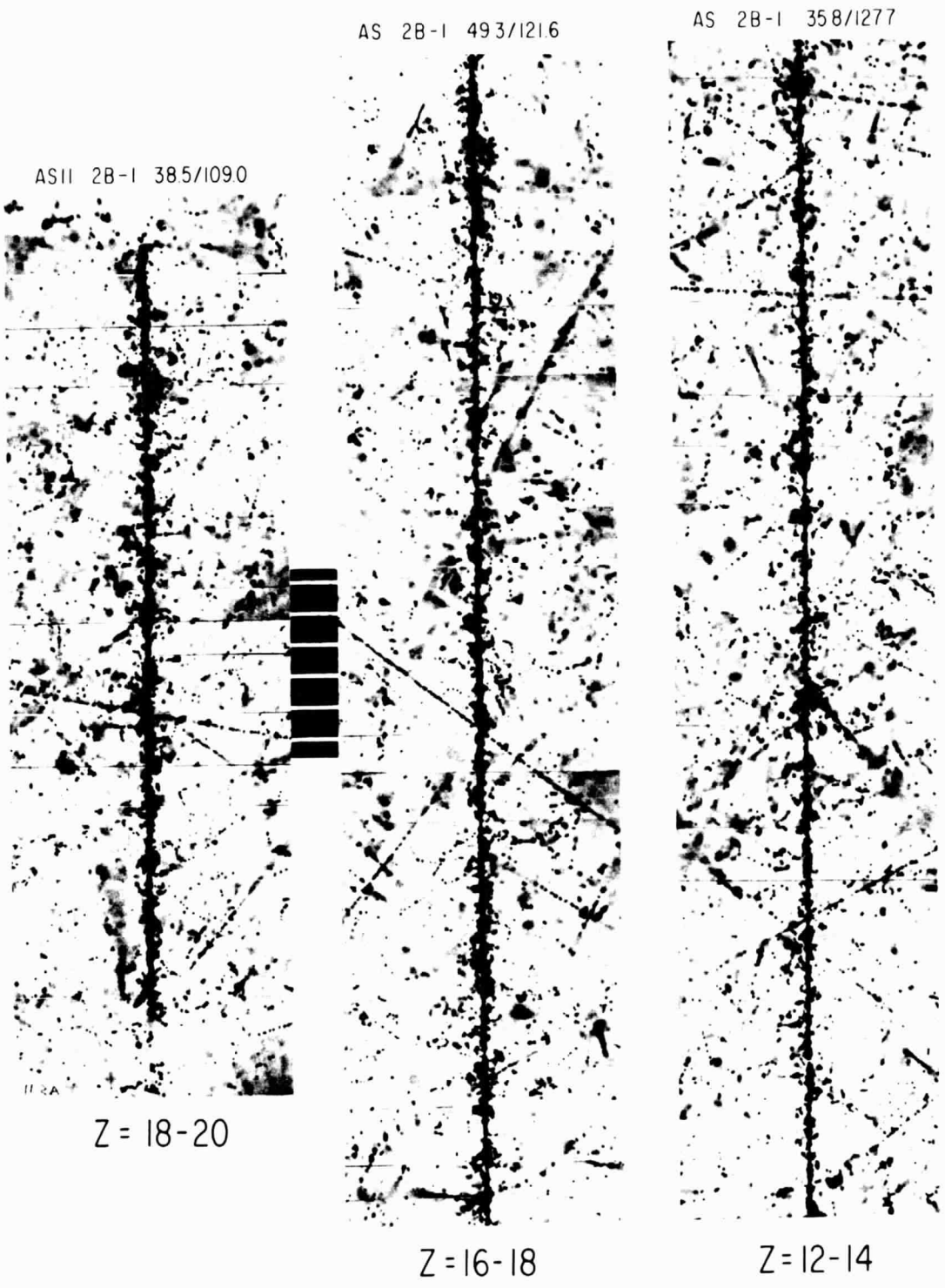

HZE Particle Tracks of High Energy in 50 μ G.5 Emulsion Flown in CM Pilot's Dosimeter on Apollo-Soyuz

1 Div = 10 μ

Figure 7

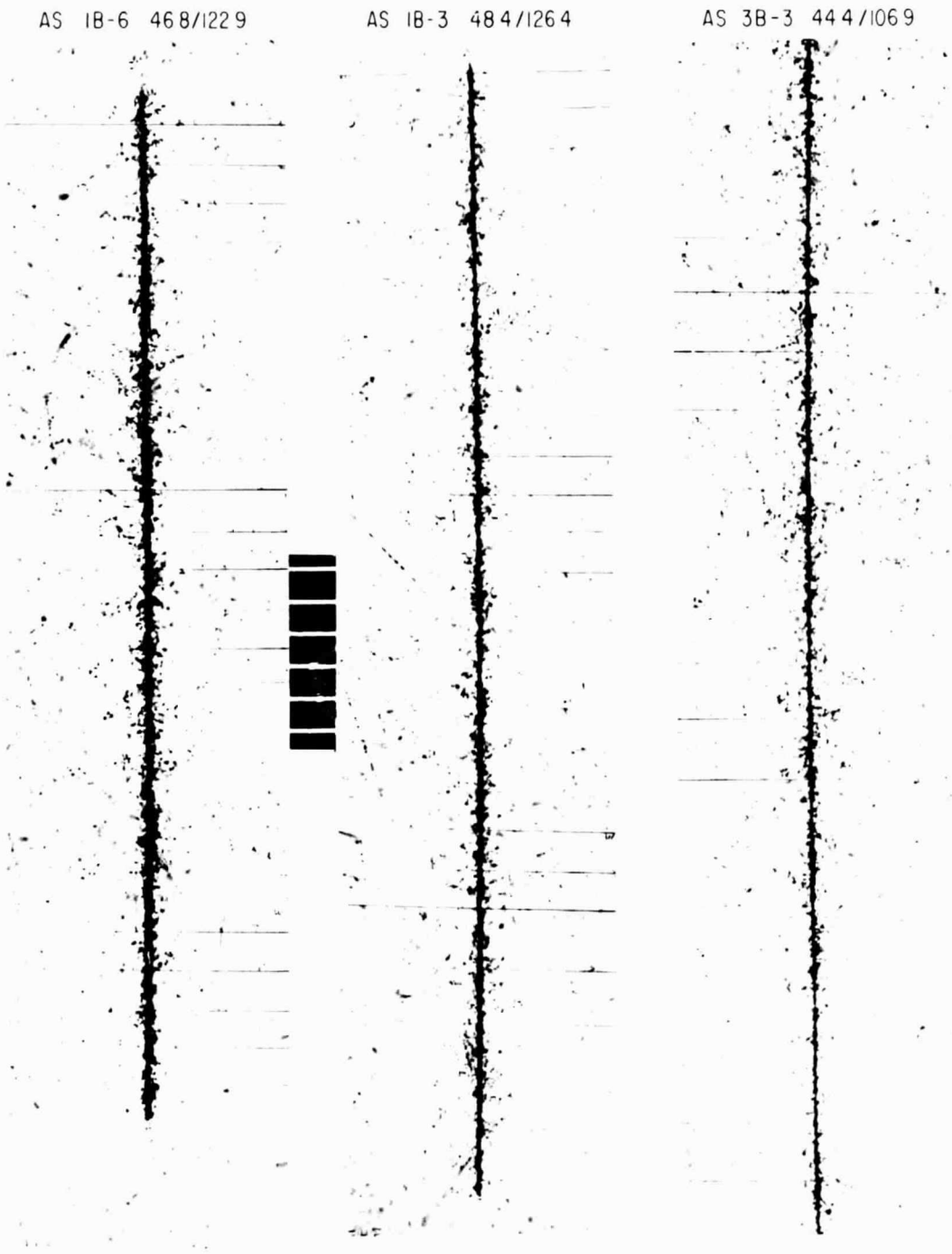

HZE Particle Tracks of High Energy in 100 μ K 2 Emulsions Flown on Apollo - Soyuz

(Left and Center : Cmdr; Right : D Pilot)

1 Div = 10 μ

Figure 8

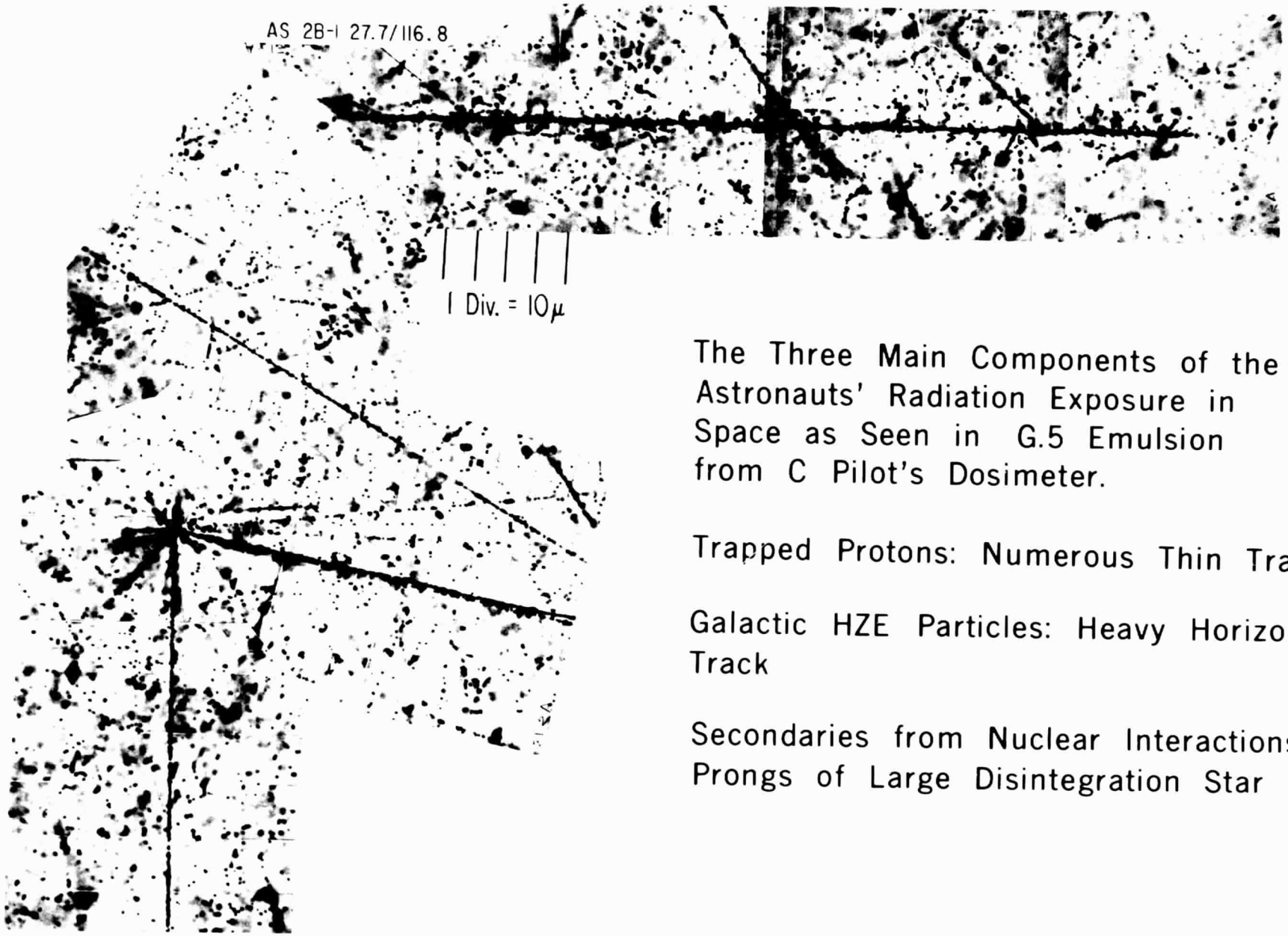

The Three Main Components of the Astronauts' Radiation Exposure in Space as Seen in G.5 Emulsion from C Pilot's Dosimeter.

Trapped Protons: Numerous Thin Tracks

Galactic HZE Particles: Heavy Horizontal Track

Secondaries from Nuclear Interactions: Prongs of Large Disintegration Star